The Time Evolution of Actual Condition and Apparent Condition for an Inspected System

Dag HORN *
* AECL Chalk River Laboratories, Chalk River, Ontario, Canada

Abstract. The actual condition of a system may not be identical to its apparent condition as reported from inspections. The apparent condition can be biased by non-detection of actual flaws, false calls of non-existent defects, incorrectly characterized indications, and lack of results from uninspected regions. Reliability analysis tools, such as probability of detection, false call estimation, and assessment of sizing uncertainty, are commonly used to compensate for the difference between the actual and apparent condition. However, these static corrections neglect the time evolution of the system condition, which may, over the system life cycle, diverge from the condition assumed by its operators.

In this work, we model the unobserved, underlying condition of a large system over decades of service life. Maintenance and repair activities, all contingent upon earlier inspection results, are included in the model. The apparent condition at each inspection date is then calculated by filtering the underlying condition through inspection reliability analysis. In this particular case study, a large historical data set permits us to compare predicted inspection results to those obtained over many years. The assumed distribution of degradation rates, effectiveness of repair, and inspection reliability parameters can then be adjusted to provide a more accurate picture of the actual system condition.

The history and predicted future life of a system are best obtained from this type of model, which permits evaluation of alternative scenarios for inspection priorities, assessment of repair effectiveness, and meaningful planning for end-of-life or life extension.

1. Introduction

Life management requires knowledge of the actual condition of a system, which may not be identical to its apparent condition as reported from inspections. The apparent condition can be biased by non-detection of actual flaws, false calls of non-existent defects, incorrectly sized indications, and lack of results from uninspected regions. Reliability analysis tools, such as probability of detection, false call estimation, and assessment of sizing uncertainty, are commonly used to compensate for the difference between the actual and apparent condition. However, these static corrections neglect the time evolution of the system condition, which may, over the system life cycle, diverge from the condition assumed by its operators.

In this work, we model the unobserved, underlying condition of a system over decades of service life. Maintenance and repair activities, all contingent upon inspection results, are included in the model. The apparent condition at each inspection date is then calculated by filtering the underlying condition through reliability analysis. In this

particular case study, a large historical data set permits us to compare predicted inspection results to those obtained over many years. The assumed distribution of degradation rates, effectiveness of repair, and reliability parameters can then be adjusted to provide a more accurate picture of the actual system condition.

Once limits on these parameters are established, the model can be exercised to evaluate alternative inspection scenarios, assess the value of repairs, and estimate system life expectancy for various maintenance strategies.

The concept is in some ways similar to the xLPR (extremely low probability of rupture) framework [1] pursued in the United States; a major difference is our focus on the consequences of inspection and repair, rather than on probabilistic fracture mechanics, and our benchmarking to extensive historical data sets.

2. Model

The test case chosen for this model is taken from the inspection of steam generators [2]; the reference data set includes inspection results from thousands of tubes per steam generator, measured over nearly two decades. The model assumes a subset of the system has an active degradation mode and that this proceeds in a stochastic (*i.e.*, random) but monotonic fashion. The simulated system condition is updated periodically, and on some of these occasions it is subjected to inspection or repaired, with inspection reliability and repair effectiveness parameterized to generate the condition that would be apparent to observers. The simulated underlying condition and simulated apparent condition can then be tracked over time and compared to the observed condition of real inspected systems, as apparent from decades of inspection results.

Although much is known about the mechanics of the degradation mode in the test case, such refinements are not introduced to drive the simulation at this stage. Other simplifications are introduced for computational tractability:

- Flaw depth, measured in percent through-wall, is binned at 5% intervals.
- Only the deepest flaw in a tube is considered.
- A probabilistic approach is taken to permit evaluation of a distribution of possible behaviours.
- The tube coordinates and flaw location of a degradation site are not preserved; only a flaw distribution (number of tubes per flaw depth bin) is retained from each cycle.
- The probability of flaw growth per propagation cycle into the next deeper bin is a parameter in the model.
- The probability of growth by n depth bins is taken as the single-bin growth probability divided by two to the $(n\text{-}1)^{th}$ power.
- Future behaviour of any potential degradation site is assumed independent of past behaviour.

These simplifications permit use of a Markov chain, which offers many advantages, including closed-form regression to large historical data sets to obtain parameter values for degradation rates, inspection reliability, and repair effectiveness. Results presented here are from the Markov simulation. However, further work, replacing the Markov chain by a Monte Carlo approach, has already begun, and will remove the need for many of the above simplifications; it will also permit tracking of multiple individual flaw sites per tube with history- and position-dependent degradation rates.

3. Markov chain for an evolving population

The principles of Markov chain calculations for inspected systems have been illustrated elsewhere [3]. The present calculation is for progressive degradation of monotonically increasing through-wall depth. We use a 21-state Markov model, with a state vector composed of 20 evenly-spaced depth bins, each 5% through-wall in width, and one plugged state. Unlike the calculation in [3], this chain has no true "repaired" state, since plugged tubes are removed from service, not replaced. Three types of iteration cycle are available: growth, growth/inspection, and growth/inspection/plugging. For a growth cycle, the *bxb* transition matrix, $M(\lambda_{ij})$, is comprised of elements λ_{ij}, which denote the probability of going from state *i* to state *j*:

$$M_{ij} = \begin{vmatrix} 1-\lambda_{01}-\lambda_{02}-\ldots-\lambda_{0b} & \lambda_{01} & \lambda_{02} & \cdots & \lambda_{0b} \\ 0 & 1-0-\lambda_{12}-\ldots-\lambda_{1b} & \lambda_{12} & \cdots & \lambda_{1b} \\ 0 & 0 & 1-\lambda_{20}-0-\ldots-\lambda_{2b} & \cdots & \lambda_{2b} \\ \vdots & \vdots & \vdots & \vdots & \vdots \\ 0 & 0 & 0 & \cdots & 1-0-0-0-\cdots \end{vmatrix}$$

.

In the calculation, *b* is the number of bins, in this case 21, and the probability of going to a deeper state (matrix elements above the diagonal) is taken as $\lambda_{ij} = \varepsilon / 2^{n-1}$, where ε is the single-bin transition probability and $n = j - i$. Reverting to a shallower state would only be possible for a complete repair. Since plugged tubes are removed from service, and are not replaced, below-diagonal elements are always zero. The diagonal elements of the matrix are the probability for remaining in the same state, and are one minus the other elements in the row, so the sum of elements in a row always adds to unity. In a cycle with no plugging, there is zero probability of going to state *j* = 21, making all off-diagonal elements of the final column in the matrix equal to zero.

For a growth/inspection/plugging cycle, the final column is the probability of detection for state *i*, with a decision level set at the plugging threshold. The remainder of the matrix is the same as for the simple growth case, but with inclusion of the plugging probability in the row normalization to unity.

The calculation is performed on the (unobserved) total system, which starts at time t_0 with an unflawed state vector p_0, with all tubes having no flaws deeper than 5%, i.e. $p_0 = [1,0,0,...,0]$. The 21x21 transition matrix $M(\lambda_{ij})$ multiplies the successive 21-element state vectors at each time, t_k, to obtain the state vector at the next operating cycle, t_{k+1}. To obtain the observed flaw distribution, each element of p_i is multiplied by the detection probability for that depth bin, calculated with the decision level for indication reporting.

4. Data

The historical inspection data with which this test case is compared comes from inspections of steam generator tubing from a nuclear power station. With statistics on the order of 10^4 tubes inspected many times each, over a period of nearly two decades, the data set is rich and comprehensive. At this stage of the model development, minor changes in detection and sizing techniques, post-remediation data (taken after the degradation mechanism was addressed), and plugging campaigns involving very few tubes are neglected. For comparison with the simulations, only flaw distributions as a function of depth and time are retained.

5. Simulating the static condition of the system

An example of a flaw depth distribution measured for one steam generator in one inspection is plotted as the discrete points in Figure 1. The inspection technology does not detect very small flaws, and the life-management strategy employed by the utility calls for plugging tubes with flaws exceeding a certain depth. Hence, a fairly narrow range of flaw depths is seen in any inspection, typically ranging from 10 to 40% through-wall depth. Plugged tubes are tallied at the arbitrary depth of 101% in the plot. The static case is presented here simply to illustrate the relationship between observed and underlying distributions. We consider the low-end data cutoff to result from application of a probability of detection curve as shown schematically by the green dashed line in the figure, and the high-end cutoff to result from a similarly shaped curve (red dashed line) with a decision threshold related to the plugging criterion. To obtain a curve corresponding to the data, a flaw distribution obtained from parameterized growth rate and population size is filtered by distributions for the probability of detection and the probability of plugging. In Figure 1, the broad grey line, filtered by the two distribution functions, gives the thin blue line, which approximates the data. This suggests the true (but unobserved) underlying distribution for very shallow flaws cannot be determined. With no possibility of detection and no consequences for tube integrity, the question is moot for condition monitoring, which deals only with the current properties of the system. However, for operational assessments, which address future condition, the time evolution of the system must be understood, and the distribution of nearly detectable flaws can be of relevance.

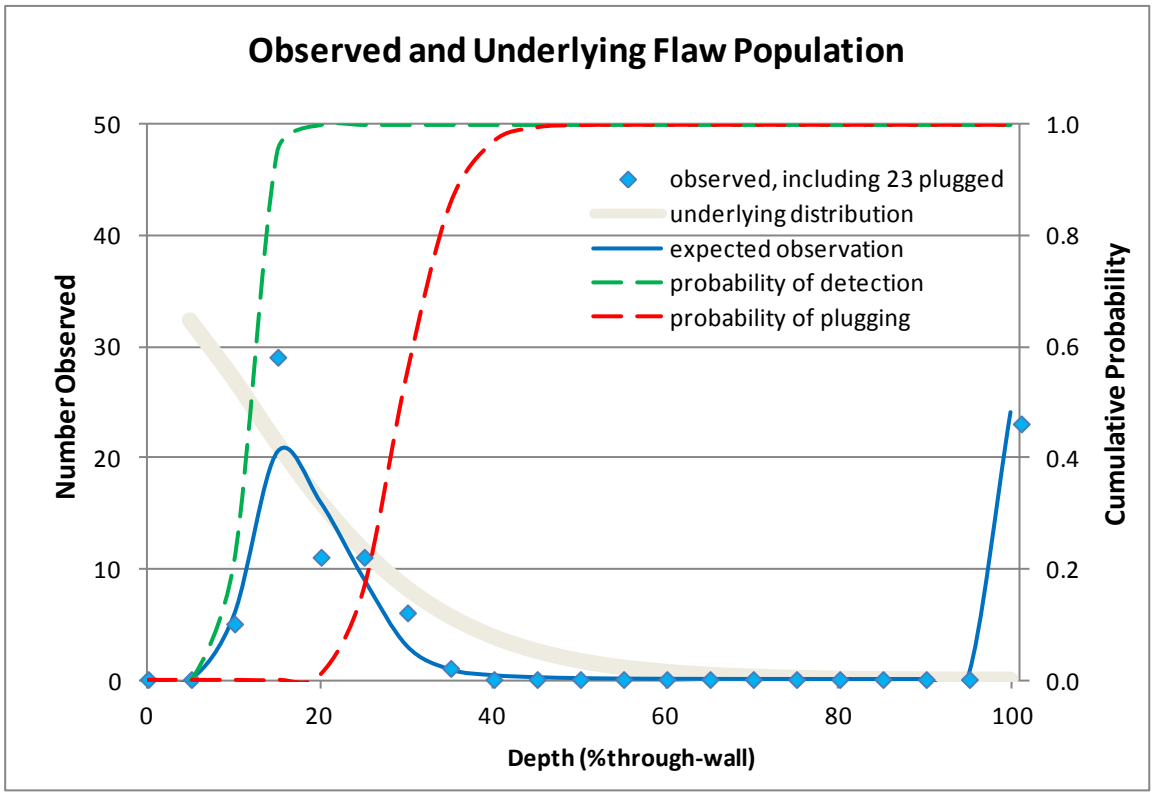

Figure 1. Number of observed flaws per 5-percent depth bin (diamonds) for a steam generator with nearly two decades of operating history. The unobserved parent distribution (thick grey line) is filtered by the detection and plugging probabilities to approximate the data, giving the thin blue line. Plugged tubes are assigned a depth of 101% through-wall).

6. Simulating the time evolution of the system

Since the flaw population actually evolves over the life of the system, a static snapshot of the detectable range of flaws is not adequate. Typically, new flaws initiate, become detectable, become deeper, and may eventually be removed by plugging. An understanding of how the system condition changes over time is needed to optimize inspection and repair strategies.

Successive inspection results of the type illustrated in Figure 1 are input for each steam generator and serve as reference values for the state vectors obtained from the Markov chain. The discrete points in Figure 2 represent such a historical distribution. The calculation is performed starting with an unflawed state vector, which is multiplied by the 21x21 transition matrix $M(\lambda_{ij})$ to obtain a new state vector. The calculation continues, with the resulting state vector multiplied again to produce the next vector, and so on. To obtain the observed flaw distribution for comparison with inspection results, each element of the relevant state vector is multiplied by the detection probability for that depth bin, calculated with the decision level for indication reporting. For operating cycles ending with repair or plugging, a matrix with non-zero transition probabilities to the repaired state is used.

A regression to minimize the residuals between the calculated state vectors and the observed distributions determines the parameters of the model. The probability of flaw growth, susceptible sample size, detection decision threshold, and plugging decision threshold are the fitted variables in the calculation. In addition, shape parameters for the detection and plugging curves may be optimized if they are not independently determined.

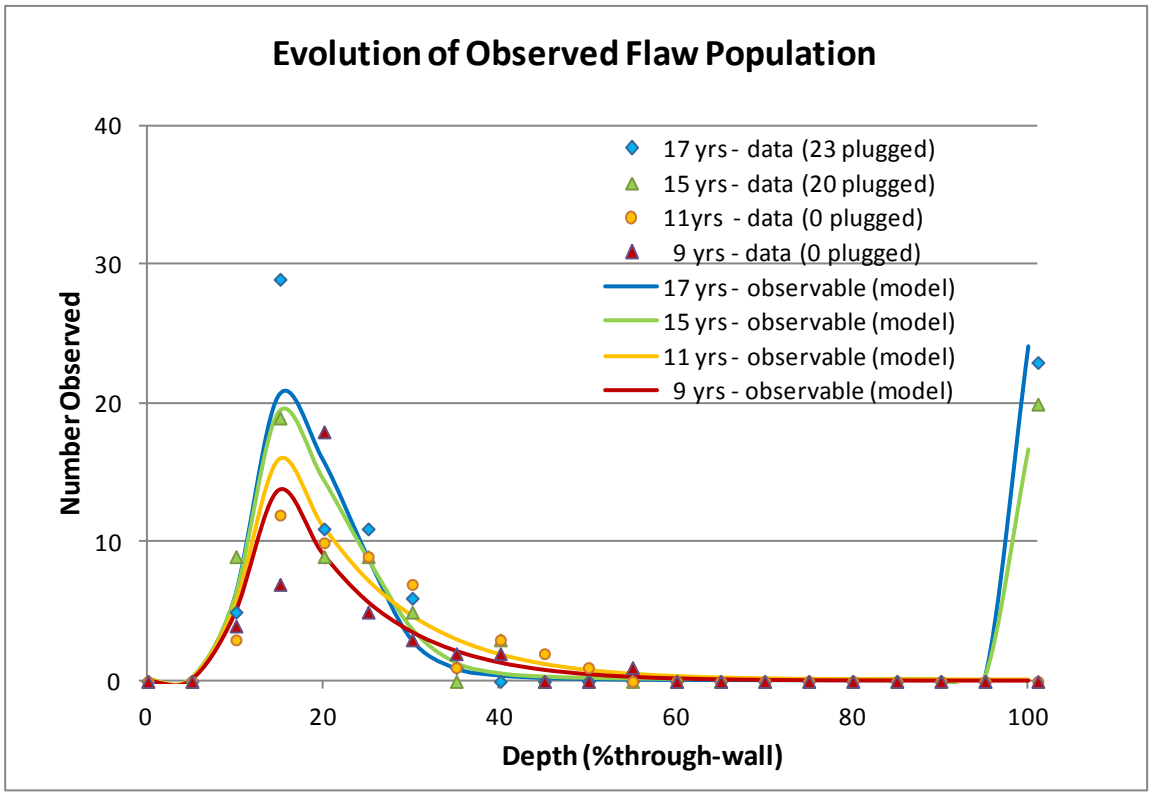

Figure 2. Time progression of the number of observed flaws per 5-percent depth bin in historical inspection data (discrete points). The smoothed lines are the calculated observable populations resulting from adjustment of flaw growth and inspection reliability parameters as chosen to approximate the data.

Figure 2 shows a superposition of the expected inspection observations on the actual data. Note the in-fill and eventual saturation of the observed flaw depth population, and the loss of the large-depth tail once the plugging option is exercised. More importantly, one can examine the modeled underlying (but incompletely observed) flaw depth distributions, on which the observable agreement is based. Figure 3 shows the progression of the underlying system condition. The link to a comprehensive set of inspection data provides confirmation of the growth and inspection reliability parameters of the simulation and supports the idea that the model may also be run forward in time, as necessary for performing operational assessments.

7. Discussion

Similar results were obtained for two other steam generators, and having obtained agreement of model and data, one can examine the resulting parameters and their physical significance.

- A consistent size is obtained for the susceptible tube population, which ranged from 165 to197, i.e., within 10% of the median value, in all three cases.
- The reporting decision level extracted from the data corresponded to 10 ± 2% through-wall depth for all three steam generators.
- The plugging decision level, also consistent, was confined to the range 27 ± 4% through-wall depth for all three steam generators.
- A variation in the apparent flaw growth rate was observed: the probability of growth into the next higher 5-percent depth bin ranged over a factor of two: from 0.04 to 0.09.

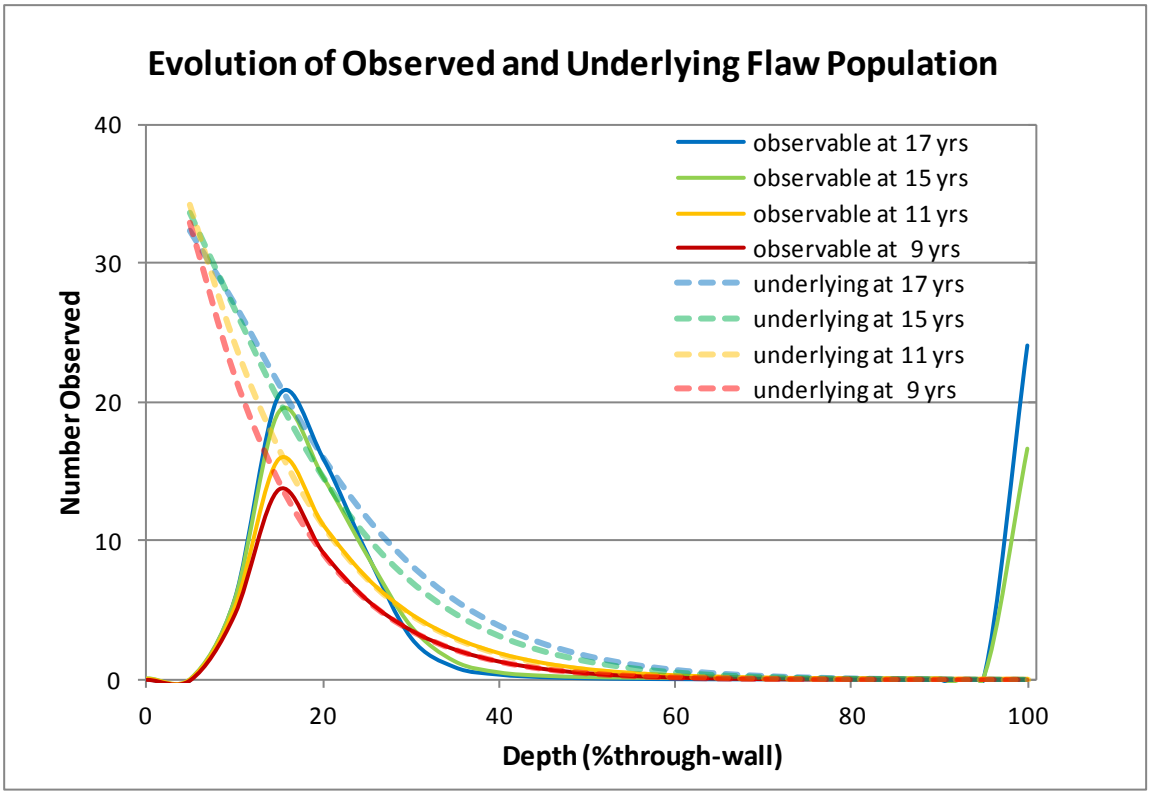

Figure 3. Progression of the observable (thin solid lines) and underlying (dashed lines) flaw population within the simulation.

A potential use for this type of analysis is to assess the effectiveness of remediation strategies. One of the steam generators examined underwent two further inspections subsequent to implementation of structural modifications. In this case, the number of flawed tubes did not increase significantly post-remediation, but this would not be meaningful *per se*, since comparison to the expected flaw number is needed. Figure 4 shows the tally of flaws deeper than 15% through-wall as a function of time. The effectiveness of the remediation can be seen from the divergence of the data (discrete points) from the growth rate modeled on the basis of the first four inspections. Further inspections would be needed to confirm effectiveness.

Further applications of the present approach may include assessment of different inspection and maintenance regimes. Longer or shorter intervals between inspection, higher or lower detection capabilities, or the acceptability of underlying system condition deduced from simulation of observable apparent condition, may provide economic or safety benefits to system operators.

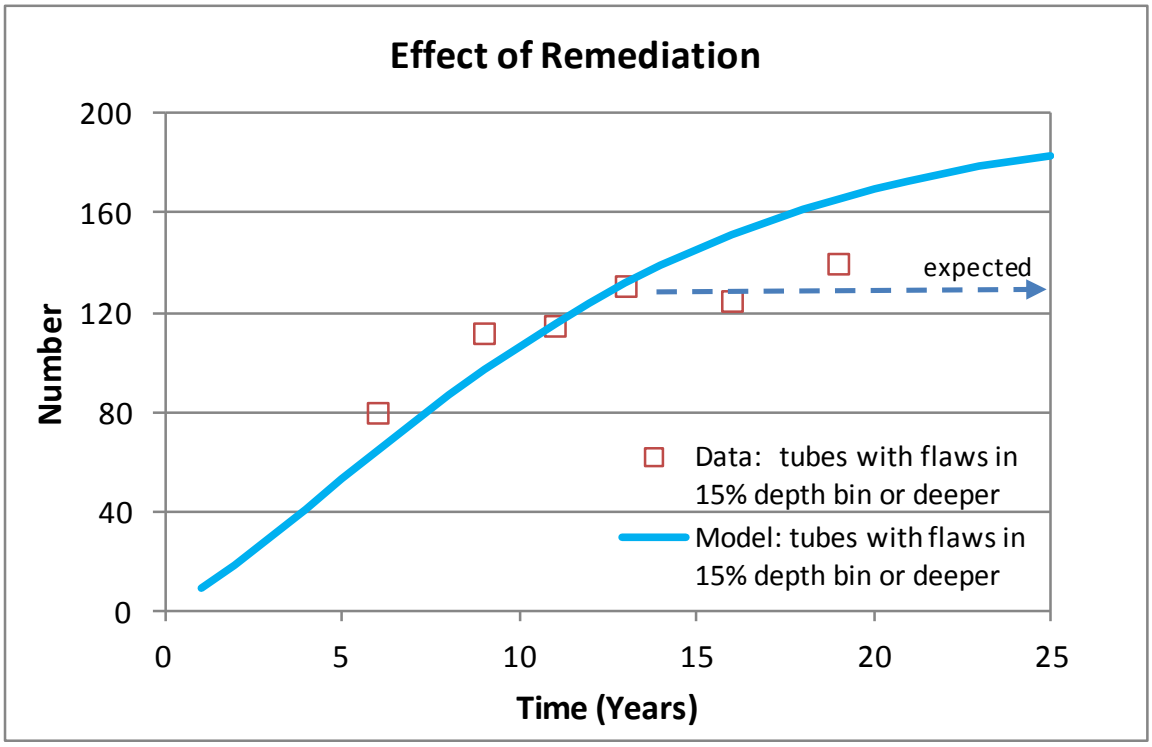

Figure 4. Effect of remediation at year 13. The model prediction and inspection data diverge in subsequent years.

8. Future Work

Limitations of the present approach include the difficulty of tracking the history of individual system elements and individual degradation sites on an element. This is due to the inherent history-independence of Markov chains and the very large matrices necessary to work around this property. A Monte Carlo approach to the problem is being undertaken to obtain more flexibility in use of model probability distributions, historical tracking of each degradation, and the ability to substitute different degradation modules into the general simulation framework.

References

[1] D. Rudland and C. Harrington, *xLPR Pilot Study Report*, NUREG 2110 (2012 May).
[2] D. Horn, *How the Condition of an Inspected and Repaired System Evolves over Time*, 4th International CANDU In-service Inspection Workshop and NDT in Canada 2012 Conference, 2012 June 18-21, Toronto, Ontario.
[3] K.N. Fleming, *Markov Models for Evaluating Risk-Informed In-Service Inspection Strategies for Nuclear Power Plant Piping Systems*, Reliability Engineering and System Safety, 83 (2004) 27.